Microchim Acta (2017) 184:1933–1940
DOI 10.1007/s00604-017-2204-5

ORIGINAL PAPER

A fluorescence based immunoassay for galectin-4 using gold nanoclusters and a composite consisting of glucose oxidase and a metal-organic framework

Xiaolong Zhang[1,2] · **Yongyi Zeng**[1,2,3] · **Aixian Zheng**[1,2] · **Zhixiong Cai**[1,2] · **Aimin Huang**[1,4] · **Jinhua Zeng**[1,2] · **Xiaolong Liu**[1,2,3] · **Jingfeng Liu**[1,2,3]

Received: 9 December 2016 / Accepted: 19 March 2017 / Published online: 29 March 2017

Abstract The authors describe a fluorescence immunoassay for galectin-4, a candidate biomarker for various cancers. Glucose oxidase was encapsulated into a zeolitic imidazolate framework to give a composite (GOx/ZIF-8 composite) that acts as a signal-transduction tag via a biomimetic mineralization process. After modification of the composite with streptavidin, it binds biotinylated antibody against galectin-4. In the immunoassay, the response to galectin-4 results from the enzymatic oxidation of glucose. This reaction produces hydrogen peroxide (H_2O_2) that reacts with iron(II) ions to generate hydroxy radical (•OH), which leads to the quenching of the fluorescence of gold nanoclusters (AuNCs). Accordingly, the fluorescence quenching of AuNCs depends on the concentration of target galectin-4. The GOx/ZIF-8 composite has a high loading capacity for GOx at uncompromised enzymatic activity. The fluorescence of AuNCs is sensitively quenched by •OH radicals. Galectin-4 can be detected by this method in concentrations as low as 10 pg·mL^{-1}. It is expected that this kind of enzyme/MOF composite-based immunoassay has a wide scope in that it may be adapted to other low-abundance proteins and biomarkers.

Keywords Zeolitic imidazolate framework · Hydrogen peroxide · Glucose · Hydroxy radical · Reactive oxygen species · BiomarkerXiaolong Zhang and Yongyi Zeng are contributed equally to this work.

Xiaolong Zhang and Yongyi Zeng are contributed equally to this work.

Electronic supplementary material The online version of this article (doi:10.1007/s00604-017-2204-5) contains supplementary material, which is available to authorized users.

✉ Xiaolong Liu
xiaoloong.liu@gmail.com

✉ Jingfeng Liu
drjingfeng@126.com

[1] The United Innovation of Mengchao Hepatobiliary Technology Key Laboratory of Fujian Province, Mengchao Hepatobiliary Hospital, Fujian Medical University, Fuzhou 350025, People's Republic of China

[2] The Liver Center of Fujian Province, Fujian Medical University, Fuzhou 350025, People's Republic of China

[3] Liver Disease Center, The First Affiliated Hospital, Fujian Medical University, Fuzhou 350005, People's Republic of China

[4] Department of Pathology, School of Basic Medical Science, Fujian Medical University, Fuzhou 350004, People's Republic of China

Introduction

Galectin-4, a member of the galactose binding lectin family, is composed of two carbohydrate recognition domains within the same peptide chain. It has been reported that Galectin-4 was involved in the regulation of cell apoptosis and the promotion of tumor metastases during cancer development and progression [1, 2]. The aberrant expression of galectin-4 has been found in several cancers, such as colorectal cancer, breast cancer, pancreatic adenocarcinomas, hepatocellular carcinoma, and gastric cancer [3, 4]. Therefore, Galectin-4 might be a promising diagnostic biomarker and a valuable therapeutic target for effective cancer treatment.

Up to now, antibody-antigen recognition and lectin-carbohydrate interaction have been exploited for the sensitive and selective detection of galectin-4 [2, 5]. Among them, enzyme-linked immunosorbent assay (ELISA) based on antibody-antigen recognition has attracted significant interests due to the specificity of antibody to antigen. In such detection systems, the key issue for signal amplification is to enhance the ratio between enzymes and target molecules. One of the effective approaches is to utilize nanomaterials as the carriers

of enzymes and detection antibodies to improve the loading content and thus accumulate the product of the enzymatic reaction [6–8]. Nowadays, various nanostructures or nanocarriers have been fabricated for this purpose, such as magnetic beads [9], metal nanoparticles [10, 11], graphene oxide [12, 13], and carbon nanotubes (CNTs) [14]. However, these nano-amplification technologies are often limited by the complicated and labored assembly processes, as well as relatively poor stability of biofunctionalized nanomaterials. It is still of great importance to explore efficient and cost-effective strategies for the fabrication of enzyme-immobilized nanoparticles with improved stability for the enhancement of sensitivity and selectivity of ELISA.

Metal-organic frameworks (MOFs) are crystalline porous compounds constructed of metal ions and organic linkers. They have hold great promise for the potential applications in gas separation and storage, catalysis, sensing, chemical separation, and drug delivery [15–17]. Currently, a series of biomacromolecules such as proteins, DNA, and enzymes are found to enable to induce the coating of protective metal-organic framework to form biomacromolecule/MOF composites [18, 19]. The resulting biocomposites offer several advantages such as high biological activities, stable under harsh conditions, and low cost synthesis steps. To the best of our knowledge, there are only a few analytical applications of the protein/MOF composites [20, 21]. Fluorescent nanomaterials have received much attentions in the field of sensing, imaging, and light emitting devices, including quantum dots [22], metal nanoclusters [23], and carbon nanomaterials [24]. It has been reported that the strong fluorescence of gold nanoclusters (AuNCs) can be effectively quenched by hydrogen peroxide (H_2O_2) and highly reactive oxygen species (hROS) including •OH, ClO^-, and $ONOO^-$ [25–27]. Since •OH can be obtained from the Fenton's reaction between H_2O_2 and iron(II) ions (Fe^{2+}), the constituted AuNCs-iron(II) system can be used to detect H_2O_2 and H_2O_2-related oxidases. In this work, we combined enzyme/MOF composites with AuNCs-iron(II) system to construct a fluorescence immunoassay for the high sensitive detection of galectin-4.

Experimental

Materials and reagents

Gold(III) chloride trihydrate ($HAuCl_4 \cdot 3H_2O$), zinc acetate dihydrate, and H_2O_2 were purchased from Sinopharm Chemical Reagent Co., Ltd. (Shanghai, China, www.reagent.com.cn). Glutathione (GSH), GOx, and streptavidin were purchased from Shanghai Sangon Biological Reagent Company (Shanghai, China, www.sangon.com). Recombinant human galectin-4 protein and human galectin-4 biotinylated antibody were purchased from R&D Systems (www.rndsystems.com/cn). Glypican-3 (GPC-3), recombinant human galectin-1 and galectin-3 were purchased from Sino biological Inc. (China, www.sinobiological.com). α-fetoprotein (AFP) was purchased from Linc-Bio Science Company (Shanghai, China, www.linc-bio.com). Ferrous sulfate and 2-methylimidazole (HmIm) were obtained from Aladdin Reagent Co. Ltd., (Shanghai, China, www.aladdin-e.com). Bovine serum albumin (BSA), human serum albumin (HSA), glucose, and Tween 20 were purchased from Sigma-Aldrich Chemical Co. (USA, www. sigmaaldrich.com). 96-Well polystyrene plates were obtained from Corning Costar (Corning, New York, USA, www.corning.com/cn). Deionized water (Milli-Q grade, Millipore, www.merckmillipore.com) with a resistivity of 18.2 MΩ·cm was used throughout this study. All other reagents were of analytical reagent grade and used without further purification.

Preparation of AuNCs

The AuNCs were prepared by using GSH as the reducing-cum-protecting agent according to the previous literatures [28]. Typically, freshly prepared aqueous solutions of $HAuCl_4$ (4 mM, 2.5 mL) and GSH (8 mM, 2.5 mL) were mixed under vigorous stirring at room temperature. After 5 min, the mixture solution was heated to 70 °C for 24 h. The solution was further dialyzed using a MWCO membrane (1000 Da) in deionized water for 24 h to remove the unreacted molecules. A light yellow aqueous solution was obtained and stored in the dark at 4 °C for further usage.

Measurement of H_2O_2 and GOx activity in the AuNCs-iron(II) system

100 μL H_2O_2 with various-concentration were mixed with 78 μL of water and then 20 μL of AuNCs were added, followed by the addition of 2 μL of 1 mM Fe^{2+} solution. After incubation at room temperature for 2 min, the solution fluorescence spectra were recorded upon being excited at 375 nm. Fig. 1a displays the assay mechanism of the AuNCs for the detection of GOx activity. Briefly, 10 μL of GOx with the specified concentration (0–10 $\mu g \cdot mL^{-1}$) were incubated with glucose (5 mM) solutions, and the resulting solution was incubated for 20 min at 35 °C. Then the reaction solutions were tested following the procedure for H_2O_2 detection.

Preparation of GOx/ZIF-8-PDA-STV composite

In a typical experiment, an aqueous solution containing HmIm (160 mM, 5 mL) and GOx (2.5 mg, 500 μL) were mixed with a separate aqueous solution of zinc acetate (40 mM, 5 mL) and stirred at room temperature for 30 min [19]. The mixture solution instantaneously turned from transparent to opaque. The solution was recovered by centrifugation at 8000 rpm for

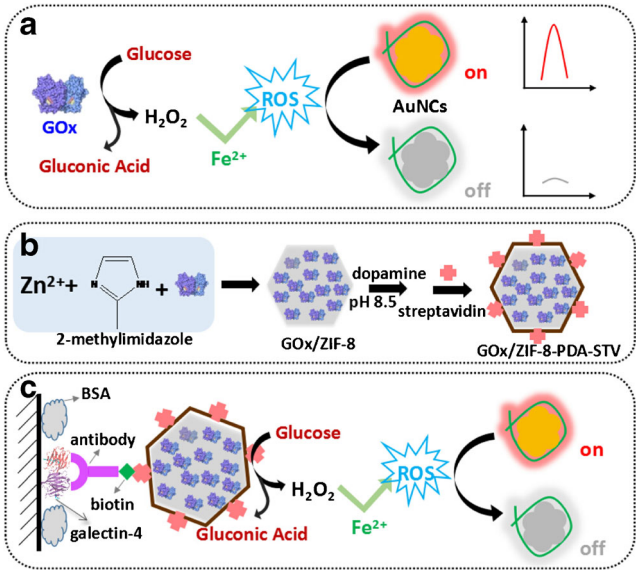

Fig. 1 Schematic illustration of (**a**) monitoring of GOx activity based on AuNCs-iron(II) system, (**b**) preparation of GOx/ZIF-8-PDA-STV composite, and (**c**) GOx/ZIF-8-based fluorescence immunoassay for the galectin-4 detection

10 min, washed with water for three times and freeze-dried. The resulting GOx/ZIF-8 composite (5 mg) was re-dispersed in 2 mL water. For coating of the PDA shell, 200 μL GOx/ZIF-8 composite solution was incubated in the freshly prepared dopamine (0.5 mg·mL^{-1}) in Tris-HCl buffer (10 mM, pH 8.5) under shaking for 1 h at room temperature. The solution was then centrifuged to remove unreacted reagents. The GOx/ZIF-8-PDA composite was linked with streptavidin by incubating with streptavidin (1 mg·mL^{-1}, 2 μL) in Tris-HCl buffer (10 mM, pH 8.5) overnight with gentle stirring [29]. After centrifuging, the GOx/ZIF-8-PDA-STV composite was resuspended into 200 μL 0.1 wt% BSA and stored at 4 °C until use.

The procedure of GOx/ZIF-8-based fluorescence immunoassay for galectin-4

The immunoassay detection was performed as the following steps. Firstly, the microplate was coated with 50 μL of galectin-4 with different concentrations in coating solution (0.05 M sodium carbonate buffer, pH 9.6) at 4 °C overnight. After rinsing with phosphate buffer (PB) for 3 runs, 300 μL 1% BSA in PB was added into each well as blocking agent and incubated at 37 °C for 2 h. After that, 50 μL of biotinylated galectin-4 detection antibody (500 ng·mL^{-1}) were added to each well. The plate was incubated at 37 °C for another 1 h, followed by washing with PBST buffer (10 mM PB, 8 g·L^{-1} NaCl, 0.2 g·L^{-1} KCl and 0.05% (*v*/v) Tween-20, pH 7.4) for three rounds. Then, 50 μL of GOx/ZIF-8-PDA-STV composite (~50 μg·mL^{-1}) solution was added into each well, and incubated at 37 °C under shaking for 1 h. The plate was washed three times, and 100 μL of glucose (5 mM) solution was added to each well for 20 min at 35 °C. Finally, the reaction solution was tested following the procedure for H_2O_2 detection.

The fluorescence intensity at 610 nm was used to evaluate the performance of this method. To investigate the selectivity of the assay, galectin-1, galectin-3, GPC-3, AFP and HSA as control proteins were analyzed respectively by this assay under the same conditions used for galectin-4 detection.

The preparation of cell lysates

Human hepatocellular carcinoma cells (MHCC97L) were kind gifts from the Second Military Medical University of China (Shanghai, China) and cultured in DMEM medium supplemented with 10% FBS, 100 U·mL^{-1} penicillin, and 100 μg·mL^{-1} streptomycin at 37 °C in a humidity atmosphere (5% CO_2). The galectin-4 is highly expressed in MHCC97L cells. To reduce its expression, shRNA (shGal4, 5′-GGAA AGTCCCCGTTTATGAAA-3′) targeted for galectin-4 were transfected into the MHCC97L cells using Lipofectamine 2000 according to the manufacturer's instructions. After 6 h of transfection, the culture medium was replaced by fresh DMEM and the cells were further cultured for 48 h. After that, transfected and control cells were lysed in NP40 Buffer (50 mM Tris-HCl, pH 8.0, 150 mM NaCl, 1 mM EDTA, 1% NP40) containing protease inhibitor cocktail (Thermo Scientific, www.thermo.com.cn) for 10 min on ice. The cell lysates were centrifuged at 4 °C for 15 min to remove insoluble materials. After boiling for 5 min, the supernatant was analyzed by SDS-PAGE and Western blot analysis with anti-β-actin and anti-galectin-4 antibodies.

Results and discussion

Principle of GOx/ZIF-8-based fluorescence immunoassay

Fig. 1a illustrates a phenomenon that the fluorescence of AuNCs is quenched in the presence of glucose oxidase (GOx) and Fe^{2+}. We noted that GOx-catalyzed oxidation of β-D-glucose leads to the formation of H_2O_2. The generated H_2O_2 can react rapidly with Fe^{2+} to produce •OH, which leads to the fluorescence quenching of AuNCs. Thus, the AuNCs-iron(II) system can be performed for monitoring of GOx activity. To employ the above phenomenon into immunoassay, streptavidin-modified GOx/ZIF-8 composite (GOx/ZIF-8-PDA-STV composite) as signal-transduction tag was first prepared. The synthesis route is shown in Fig. 1b. Firstly, numerous GOx were encapsulated into the ZIF-8 MOFs via a biomimetic mineralization process. Then the formed GOx/ZIF-8 composite was coated with polydopamine (PDA) on its surface, and finally streptavidin was immobilized on the PDA shell by Michael addition or Schiff base reaction. Fig. 1c displays the schematic representation of the GOx/ZIF-8-based

fluorescence immunoassay toward target galectin-4. When target protein galectin-4 is present on the microplate, it binds specifically biotinylated anti-galectin-4 detection antibody. And then GOx/ZIF-8-PDA-STV composite was connected to biotinylated antibody to result in an antibody-GOx/ZIF-8-PDA-STV composite. So, the amount of the connected composites is related to the concentration of galectin-4. When in the presence of glucose and Fe^{2+}, the fluorescence of AuNCs is quenched, which in turn can be used to quantify the detection targets. Since GOx/ZIF-8-PDA-STV composite can react with any biotinylated biomolecules through a biotin-streptavidin interaction, the immunoassay is expected to provide a sensitive platform for the detection of most of target proteins and biomarkers.

Synthesis and characterization of AuNCs

The AuNCs were synthesized using GSH as reducing-cum-protecting agent following the previous reports [28]. The size of AuNCs is about 2–4 nm, as shown in TEM image (Fig. S1). The spectroscopic properties of AuNCs were also studied (Fig. 2). There is a shoulder peak at about 400 nm in the UV-vis spectrum of AuNCs, while the fluorescence emission spectrum shows a band centered at about 610 nm upon excitation at 375 nm. These characteristics are well matching with those reported in the literatures for AuNCs [28], which confirms the successful synthesis of AuNCs.

Measurement of H_2O_2 and GOx activity in the AuNCs-iron(II) system

Among various hROS, •OH is considered as the most effective fluorescence quencher of AuNCs. The •OH can be produced by the Fenton reaction ($Fe^{2+}+H_2O_2 \rightarrow Fe^{3+}+ \bullet OH + OH^-$) through simply mixing ferrous ions with H_2O_2. Hence, we employed •OH as a model hROS. The fluorescence response of AuNCs to •OH was depicted in Fig. 3a. In the presence of Fe^{2+} and H_2O_2, the fluorescence of AuNCs was strongly quenched (by ~80%), which suggests the highly sensitive responsiveness of AuNCs to •OH. In a control experiment, using only Fe^{2+} or H_2O_2 shows negligible effect on the fluorescence intensity. This result is consistent with those described in the literatures [25, 30]. Based on the sensitive fluorescence quenching in response to •OH, AuNCs can be chose as a promising probe for H_2O_2 detection. Upon addition of H_2O_2 with different concentrations into the AuNCs-iron(II) system, the fluorescence at 610 nm decreased with the increasing H_2O_2 level in the solutions (Fig. 3b). This system allows for the detection of H_2O_2 at concentration as low as 0.2 μM (Fig. 3c). The results indicate the feasibility of AuNCs-iron(II) system to measure H_2O_2 quantitatively.

The enzymatic activity of GOx can be evaluated in the AuNCs-iron(II) system based on the GOx-catalyzed oxidation of glucose to produce H_2O_2. To verify the viability of the design to monitor GOx activity, several control tests were performed, the results are recorded in Fig. 4a. As expected, the fluorescence intensity of AuNCs obviously decreased after the addition of both GOx and glucose (curve d in Fig. 4a). For comparison, when GOx or glucose was absent in the detection system, almost no fluorescence change can be measured (curve b and c in Fig. 4a). The following parameters were optimized: (a) Temperature and (b) Catalytic time. Respective data and figures are given in the Electronic Supporting Material. We found the following experimental conditions to give best results: (a) A temperature of 37 °C (Fig. S2) and (b) Catalytic time of 20 min (Fig. S3). Under the optimized reaction conditions, we observed that the fluorescence intensity of AuNCs was highly related to the concentration of GOx (Fig. 4b, c). As low as 0.02 $\mu g \cdot mL^{-1}$ GOx can be detected. It demonstrates the potential of AuNCs for sensitive detection of H_2O_2-related oxidases.

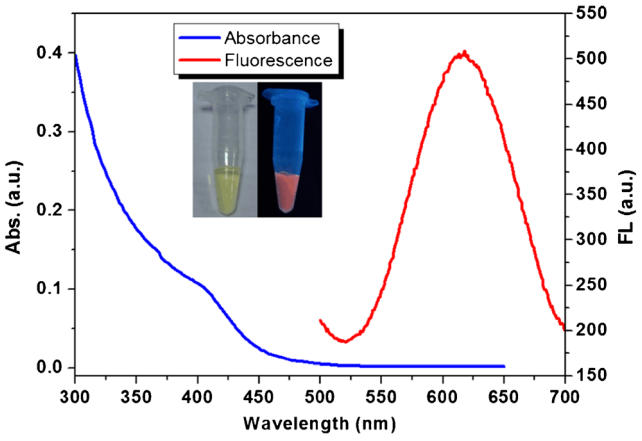

Fig. 2 The UV-vis (blue) and fluorescence emission (red) spectra of AuNCs. Inset: photograph of AuNCs under daylight and UV light illumination. Excitation and emission wavelengths of AuNCs is 375 nm and 610 nm

Fabrication and evaluation of GOx/ZIF-8-PDA-STV composite

Owing to the good responsive behavior of GOx toward the AuNCs-iron(II) system, we attempted to introduce this approach into immunoassay. We synthesized the GOx/ZIF-8-PDA composite as signal probe. The GOx/ZIF-8 composite was prepared by simply mixing 2-methylimidazole solution, zinc acetate solution and GOx together at room temperature for 30 min. In the growth process, GOx was applied to induce the ZIF-8 coating formation and simultaneously encapsulated into the ZIF-8 with almost maintenance of bioactivity [19, 31]. For the purpose of the streptavidin modification, the GOx/ZIF-8 composite was incubated with dopamine in weak alkaline buffer to form PDA shell on its surface. The TEM

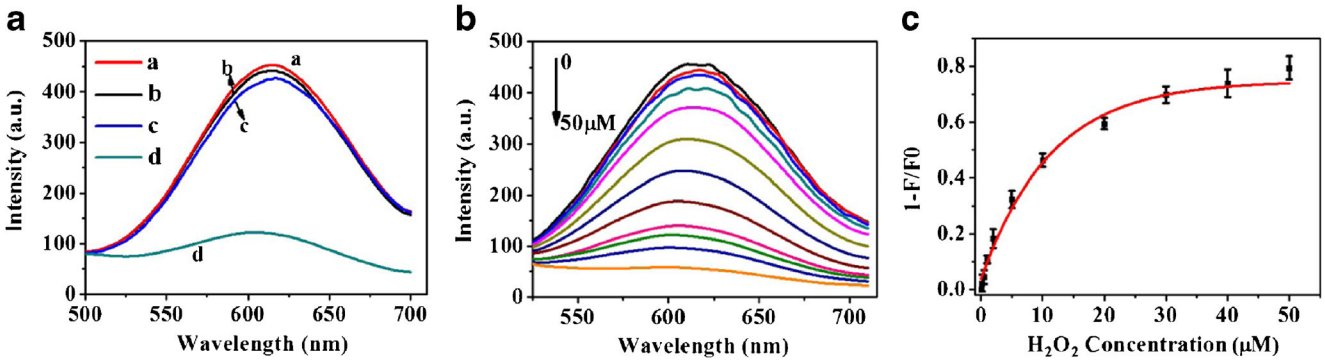

Fig. 3 **a** The fluorescence intensity of a) AuNCs, b) AuNCs +10 μM Fe^{2+}, c) AuNCs +20 μM H_2O_2, and d) AuNCs +10 μM Fe^{2+}+20 μM H_2O_2. **b** The fluorescence intensity of AuNCs in the presence of 10 μM Fe^{2+} and H_2O_2 (0, 0.2, 0.5, 1, 2, 5, 10, 20, 30, 40, 50 μM). **c** The 1-F/F0 values were plotted against various concentrations of H_2O_2. F0 and F are the emission fluorescence intensities of AuNCs at 610 nm in the absence and presence of H_2O_2. Error bar: standard deviations of three independent measurements

images in Fig. S4 exhibit the morphology of GOx/ZIF-8 composite and GOx/ZIF-8-PDA composite. The size of GOx/ZIF-8-PDA composite ranges from 400 nm to 600 nm. And a grey PDA shell with well-defined configuration and homogeneity is readily observed on the surface of GOx/ZIF-8 composite. Fourier transform infrared spectroscopy (FTIR) was employed to ascertain the entrapping of enzyme GOx into ZIF-8. In the FTIR spectrum (Fig. S5), both GOx/ZIF-8 composite and GOx/ZIF-8-PDA composite showed stretches characteristic of GOx at ~1640–1660 cm^{-1}, which is mainly attributed to C = O stretching mode of amide I [32]. The powder X-ray diffraction (PXRD) measurement indicates that the crystallinity of the GOx/ZIF-8 composite is unchanged compared to that of ZIF-8 (Fig. S6). Moreover, from the photograph shown in Fig. S7, the GOx/ZIF-8 composite presents light yellow, which is the characteristic color of GOx, rather than the pure white of ZIF-8. After the coating of PDA, the color of composite turns from light yellow to black. This fact confirms again the successful synthesis of GOx-encapsulated ZIF-8 composite.

Activity loss often causes the reducing of sensitivity of the enzyme immunoassays. So, it is necessary to evaluate the enzymatic activity of GOx embedded in the GOx/ZIF-8-PDA composite. As desired, the fluorescence of AuNCs was still efficiently quenched in the presence of GOx/ZIF-8-PDA composite (curve d in Fig. S8a). Conversely, no obvious fluorescence quenching occurred for the ZIF-8-PDA composite (curve c in Fig. S8a). As seen in Fig. S8b, the fluorescence of AuNCs was found to gradually decrease with increasing the concentration of GOx/ZIF-8-PDA composite. The result above is concluded that GOx embedded in the GOx/ZIF-8-PDA composite possesses high enzymatic activity and GOx/ZIF-8-PDA composite can be an appealing signal-transduction probe for immunoassays.

Analytical performance of fluorescence immunoassay for galectin-4 detection

The prepared GOx/ZIF-8-PDA composite is employed as signal-transduction tag for the detection of target galectin-4

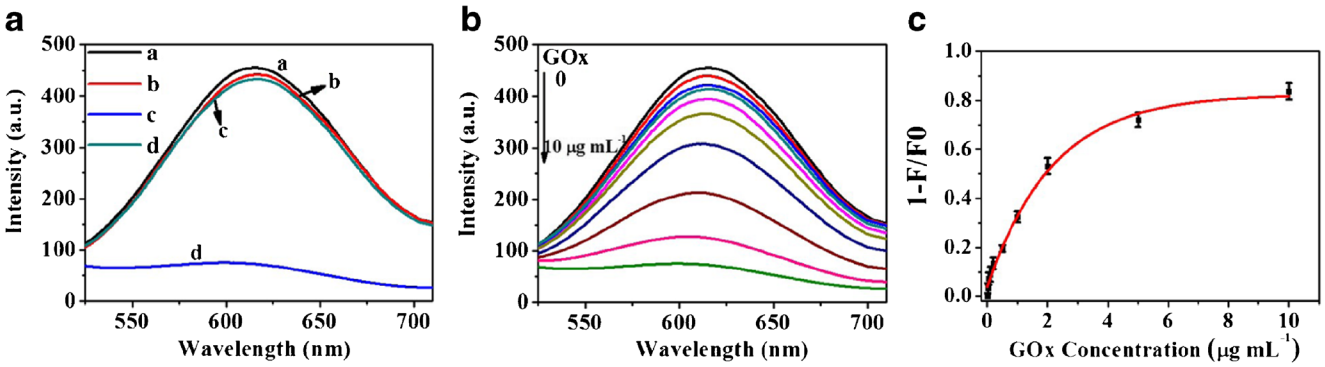

Fig. 4 **a** The fluorescence intensity of a) AuNCs, b) AuNCs +10 μM Fe^{2+} + 5 mM glucose, c) AuNCs +10 μM Fe^{2+} + 10 μg·mL^{-1} GOx, and d) AuNCs +10 μM Fe^{2+} + 5 mM glucose +10 μg·mL^{-1} GOx. **b** The fluorescence intensity of AuNCs towards different concentrations of GOx (0, 0.02, 0.05, 0.1, 0.2, 0.5, 1, 2, 5, 10 μg·mL^{-1}) in the present of 5 mM glucose and 10 μM Fe^{2+}. **c** The 1-F/F0 values were plotted against various concentrations of GOx. F0 and F are the emission fluorescence intensities of AuNCs at 610 nm in the absence and presence of GOx. Error bar: standard deviations of three independent measurements

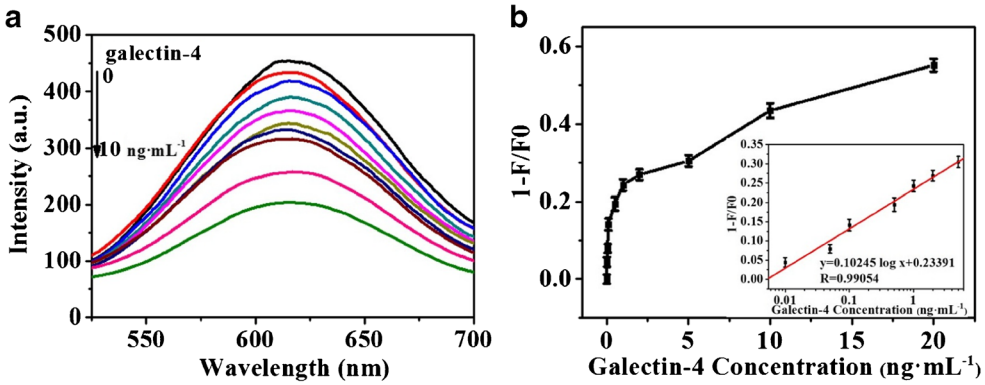

Fig. 5 **a** Fluorescence response of immunoassays with target galectin-4 with concentrations of 0, 0.01, 0.05, 0.1, 0.5, 1, 2, 5, 10, 20 ng·mL^{-1}. **b** The intensity change (1-F/F0) plotted against various concentrations of galectin-4. Inset: the resulting calibration curve of logarithm of galectin-4 concentration (range from 0 to 5 ng·mL^{-1}) with (1-F/F0). F0 and F are the emission fluorescence intensities of AuNCs at 610 nm in the absence and presence of galectin-4. Error bar: standard deviations of three independent measurements

with a single-antibody immunoassay by using the AuNCs-iron(II) system. Galectin-4 standards with different concentrations were determined by using the designed immunoassay. As shown in Fig. 5a, the fluorescence intensity of the AuNCs decreased with the increasing galectin-4 concentration from 0.01 to 20 ng·mL^{-1}. Higher concentrations of galectin-4 corresponded to higher amounts of GOx/ZIF-8-PDA composite captured in the plates, leading to produce more •OH to give a fluorescence quenching signal. By collecting the fluorescence intensity of the system at 610 nm for each solution, we obtained a calibration curve by using a curve-fitting procedure (Fig. 5b). A pseudolinear relationship between the intensity change and the logarithm of galectin-4 level can be fitted to the points from 0.01 to 5 ng·mL^{-1}, with a calibration function of $y = 0.10245logx + 0.23391$, $R = 0.99054$. It permits detection of as low as 10 pg·mL^{-1} galectin-4. Table S1 presents that the analytical properties of GOx/ZIF-8-based fluorescence immunoassay are compared with other reported methods for the galectin-4 detection. We presume that the high sensitivity is due to the effective loading of GOx in the ZIF-8 and the remarkable catalytic activity of embedded GOx. Moreover, the high sensitive responsiveness of AuNCs to •OH is also crucial to the enhanced detectable signal in the immunoassay.

To assess the selectivity of this immunoassay, selectivity experiment was performed using 1 ng·mL^{-1} of galectin-4 and 10 ng·mL^{-1} of galectin-1, galectin-3, GPC-3, AFP and HSA, respectively. The reason for the use of these non-target proteins as control is that they usually coexist in the human serum samples and may cause potential interference in the detection of galectin-4. As shown in Fig. 6, the target galectin-4 resulted in the effective quenching of the fluorescence of AuNCs because of the specificity of antibody toward its target protein. In contrast, there was no obvious responsiveness of AuNCs-iron(II) system toward the non-specific proteins even those with 10 times higher concentrations. This result clearly shows that the immunoassay exhibits high selectivity toward the target protein. Furthermore, the GOx/ZIF-8-PDA composite can be implemented as a selective platform against other proteins and DNA.

Analytical applications in real samples

To verify the applicable potential of the fluorescence immunoassay for real samples, analysis of galectin-4 in cancer cell lysate was implemented. Galectin-4 is highly expressed in MHCC97L cells. RNAi experiments for gene silencing were carried out to knock down the endogenous expression of galectin-4. From the Western blot analysis depicted in the inset of Fig. 7, the expression of galectin-4 was obviously reduced after gene silencing. The lysate of gene silenced cells and MHCC97L cells lysates with different concentrations of galectin-4 were tested in the fluorescence immunoassay. As

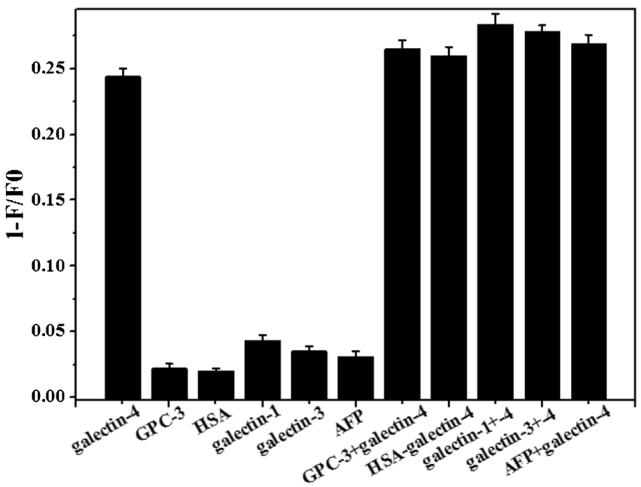

Fig. 6 Selectivity of the fluorescence immunoassay against galectin-4 (1 ng·mL^{-1}) and other non-target proteins (10 ng·mL^{-1}). F0 and F are the emission fluorescence intensities of AuNCs at 610 nm in the absence and presence of different proteins. Error bar: standard deviations of three independent measurements

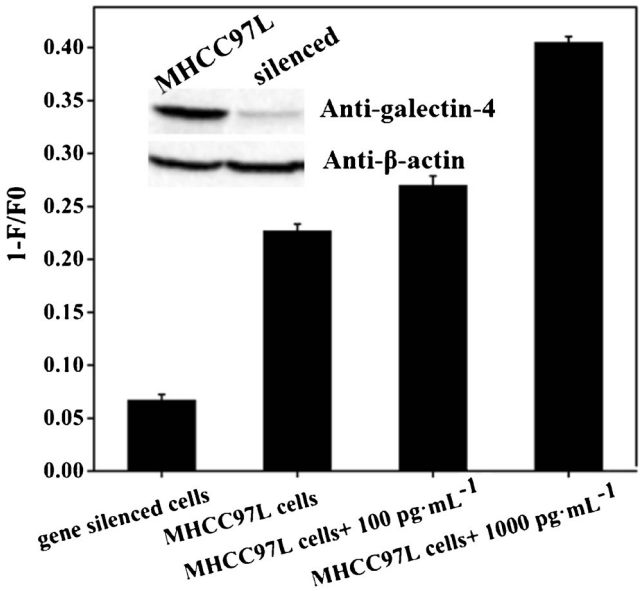

Fig. 7 Fluorescence response of immunoassays for analyzing the lysates of gene silenced cells and MHCC97L cells lysates after addition of different concentrations of galectin-4 (0, 100 pg·mL^{-1}, 1000 pg·mL^{-1}). The inset images represent the Western blot analysis of galectin-4 expression in MHCC97L cells and the gene silenced cells. β-Actin serves as a control for equal protein loading

shown in Fig. 7, MHCC97L cells lysate exhibits obviously higher signal change than that of gene silenced cells due to the higher expression of galectin-4 in MHCC97L cells. The signal change can be further enhanced with increasing the concentration of galectin-4 in MHCC97L cells lysate. These results demonstrate that this fluorescence immunoassay is capable of detecting target protein in cell lysates, showing potential application in real samples.

Conclusions

In summary, the GOx/ZIF-8-PDA composite was successfully fabricated via a biomimetic mineralization process and a polymerization reaction of dopamine. It holds significant advantages including costly preparation, good stability, and high-efficiency loading protein content. Importantly, GOx encapsulated in the MOFs displays a remarkable enzymatic activity, which has an essential role for the signal amplification. Based on it, we developed a fluorescence immunoassay using GOx/ZIF-8-PDA composites and AuNCs-iron(II) system, permitting detection of as low as 10 pg·mL^{-1} galectin-4. Beside the effective catalytic activity of GOx/ZIF-8-PDA composite, the superior sensitivity of the immunoassay can be attributed to the highly sensitive responsiveness of AuNCs to •OH. Furthermore, the immunoassay presents high selectivity towards galectin-4. Although only galectin-4 is used as a proof-of-concept, this immunoassay strategy is generalizable to be readily extended to other ELISA systems for some low-abundance proteins and biomarkers.

Acknowledgements This work is supported by the Science and Technology Infrastructure Construction Program of Fujian Province (Grant No. 2014Y2005); the specialized Science and Technology Key Project of Fujian Province (Grant No. 2013YZ0002-3); the key project of Science and Technology Department of Fujian Province (Grant No.2014Y0027); the Natural Science Foundation of Fujian Province (Grant No. 2014 J01389 and 2016 J05206); the Guiding Project of Fujian Science and Technology Department (Grant No. 2015Y0056); the Scientific Foundation of the Fujian provincial Health and Family Planning Commission (Grant No. 2015-1-95); the Scientific Foundation of Fuzhou Health Department (Grant No. 2015-S-WQ11); the Scientific Foundation of Fuzhou (Grant No. 2015-S-143-16).

Compliance with ethical standards The author(s) declare that they have no competing interests.

References

1. Liu FT, Rabinovich GA (2005) Galectins as modulators of tumour progression. Nat Rev Cancer 5:29–41
2. Barrow H, Guo X, Wandall HH, Pedersen JW, Fu B, Zhao Q, Chen C, Rhodes JM, Yu LG (2011) Serum galectin-2, −4, and-8 are greatly increased in colon and breast cancer patients and promote cancer cell adhesion to blood vascular endothelium. Clin Cancer Res 17:7035–7046
3. Huflejt ME, Leffler H (2003) Galectin-4 in normal tissues and cancer. Glycoconj J 20:247–255
4. Kim SW, Park KC, Jeon SM, Ohn TB, Kim TI, Kim WH, Cheon JH (2013) Abrogation of galectin-4 expression promotes tumorigenesis in colorectal cancer. Cell Oncol 36:169–178
5. Yoshioka K, Sato Y, Murakami T, Tanaka M, Niwa O (2010) One-step detection of galectins on hybrid monolayer surface with protruding lactoside. Anal Chem 82:1175–1178
6. Pei X, Zhang B, Tang J, Liu B, Lai W, Tang D (2013) Sandwich-type immunosensors and immunoassays exploiting nanostructure labels: a review. Anal Chim Acta 758:1–18
7. Tang J, Huang Y, Liu H, Zhang C, Tang D (2016) Novel glucometer-based immunosensing strategy suitable for complex systems with signal amplification using surfactant-responsive cargo release from glucose-encapsulated liposome nanocarriers. Biosens Bioelectron 79:508–514
8. Pal S, Bhand S (2015) Zinc oxide nanoparticle-enhanced ultrasensitive chemiluminescence immunoassay for the carcinoma embryonic antigen. Microchim Acta 182:1643–1651
9. Liu D, Yang J, Wang HF, Wang Z, Huang X, Wang Z, Niu G, Walker ARH, Chen X (2014) Glucose oxidase-catalyzed growth of gold nanoparticles enables quantitative detection of attomolar cancer biomarkers. Anal Chem 86:5800–5806
10. Lai W, Tang D, Zhuang J, Chen G, Yang HH (2014) Magnetic bead-based enzyme-chromogenic substrate system for ultrasensitive colorimetric immunoassay accompanying cascade reaction for enzymatic formation of squaric acid-iron(III) chelate. Anal Chem 86:5061–5068
11. Guo Q, Li X, Shen C, Zhang S, Qi H, Li T, Yang M (2015) Electrochemical immunoassay for the protein biomarker mucin 1 and for MCF-7 cancer cells based on signal enhancement by silver nanoclusters. Microchim Acta 182:1483–1489

12. Li J, Wu LJ, Guo SS, Fu HE, Chen GN, Yang HH (2013) Simple colorimetric bacterial detection and high-throughput drug screening based on a graphene-enzyme complex. Nano 5:619–623
13. Xu H, Wang D, He S, Li J, Feng B, Ma P, Xu P, Gao S, Zhang S, Liu Q, Lu J, Song S, Fan C (2013) Graphene-based nanoprobes and a prototype optical biosensing platform. Biosens Bioelectron 50: 251–255
14. Wang J, Liu G, Jan MR (2004) Ultrasensitive electrical biosensing of proteins and DNA: carbon-nanotube derived amplification of the recognition and transduction events. J Am Chem Soc 126:3010–3011
15. Furukawa H, Cordova KE, O'Keeffe M, Yaghi OM (2013) The chemistry and applications of metal-organic frameworks. Science 341:1230444
16. Zhang T, Lin W (2014) Metal-organic frameworks for artificial photosynthesis and photocatalysis. Chem Soc Rev 43:5982–5993
17. Silva P, Vilela SMF, Tomé JPC, Paz FAA (2015) Multifunctional metal-organic frameworks: from academia to industrial applications. Chem Soc Rev 44:6774–6803
18. Lyu F, Zhang Y, Zare RN, Ge J, Liu Z (2014) One-pot synthesis of protein-embedded metal-organic frameworks with enhanced biological activities. Nano Lett 14:5761–5765
19. Liang K, Ricco R, Doherty CM, Styles MJ, Bell S, Kirby N, Mudie S, Haylock D, Hill AJ, Doonan CJ, Falcaro P (2015) Biomimetic mineralization of metal-organic frameworks as protective coatings for biomacromolecules. Nat Commun 6:7240
20. Wu X, Ge J, Yang C, Hou M, Liu Z (2015) Facile synthesis of multiple enzyme-containing metal-organic frameworks in a biomolecule-friendly environment. Chem Commun 51:13408–13411
21. Cheng H, Zhang L, He J, Guo W, Zhou Z, Zhang X, Nie S, Wei H (2016) Integrated nanozymes with nanoscale proximity for in vivo neurochemical monitoring in living brains. Anal Chem 88:5489–5497
22. Ando M, Kamimura T, Uegaki K, Biju V, Shigeri Y (2016) Sensing of ozone based on its quenching effect on the photoluminescence of CdSe-based core-shell quantum dots. Microchim Acta 183:3019–3024
23. Chen LY, Wang CW, Yuan Z, Chang HT (2014) Fluorescent gold nanoclusters: recent advances in sensing and imaging. Anal Chem 87:216–229
24. Zhang XL, Zheng C, Guo SS, Li J, Yang HH, Chen G (2014) Turn-on fluorescence sensor for intracellular imaging of glutathione using g-C_3N_4 nanosheet-MnO_2 sandwich nanocomposite. Anal Chem 86:3426–3434
25. Chen T, Hu Y, Cen Y, Chu X, Lu Y (2013) A dual-emission fluorescent nanocomplex of gold-cluster-decorated silica particles for live cell imaging of highly reactive oxygen species. J Am Chem Soc 135:11595–11602
26. Xia X, Long Y, Wang J (2013) Glucose oxidase-functionalized fluorescent gold nanoclusters as probes for glucose. Anal Chim Acta 772:81–86
27. Jin L, Shang L, Guo S, Fang Y, Wen D, Wang L, Yin J, Dong S (2011) Biomolecule-stabilized au nanoclusters as a fluorescence probe for sensitive detection of glucose. Biosens Bioelectron 26: 1965–1969
28. Luo Z, Yuan X, Yu Y, Zhang Q, Leong DT, Lee JY, Xie J (2012) From aggregation-induced emission of au(I)-thiolate complexes to ultrabright au(0)@au(I)-thiolate core-shell nanoclusters. J Am Chem Soc 134:16662–16670
29. Yang SH, Kang SM, Lee KB, Chung TD, Lee H, Choi IS (2011) Mussel-inspired encapsulation and functionalization of individual yeast cells. J Am Chem Soc 133:2795–2797
30. Hu L, Deng L, Alsaiari S, Zhang D, Khashab NM (2014) "light-on" sensing of antioxidants using gold nanoclusters. Anal Chem 86: 4989–4994
31. Wu X, Yang C, Ge J, Liu Z (2015) Polydopamine tethered enzyme/metal–organic framework composites with high stability and reusability. Nano 7:18883–18886
32. Barth A, Zscherp C (2002) What vibrations tell us about proteins. Q Rev Biophys 35:369–430